J Therm Anal Calorim (2009) 98:73–82
DOI 10.1007/s10973-009-0376-x

Water behaviour in processed cheese spreads

DSC and ESEM study

Hela Gliguem · Dorra Ghorbel · Cécile Grabielle-Madelmont · Benoît Goldschmidt · Sylviane Lesieur · Hamadi Attia · Michel Ollivon · Pierre Lesieur

Special Chapter dedicated to the memory of dr. Michel Ollivon

Abstract The behaviour of water in two processed cheese spreads, either standard or cream-enriched, was studied by differential scanning calorimetry (DSC) in the −50 to 45 °C temperature range as a function of controlled dehydration. The results were analyzed and related to cheese microstructures observed by environmental scanning electron microscopy (ESEM). Water freezing and subsequent ice melting were found to be dependent on the cheese composition in hydrophilic components and on water confinement within the micro-domains delimited by the fat droplets. Both cheeses exhibited partial water freezing from supercooling state while ice nucleation process was shown to be tightly affected by water connectivity within the cheese matrices.

Keywords Dehydration · DSC · ESEM · Ice melting · Oil-in-water emulsion · Water crystallization

H. Gliguem · C. Grabielle-Madelmont · S. Lesieur · M. Ollivon
Equipe Physico-Chimie des Systèmes Polyphasés, UMR 8612 du CNRS, 5 rue J. B. Clément, 92296 Châtenay-Malabry, France

D. Ghorbel · H. Attia
Unité d'Analyses Alimentaires, ENIS, BPW, 3038 Sfax, Tunisia

D. Ghorbel
Département de Génie Biologique et Chimique, INSAT, Centre Urbain Nord, B.P. 676, 1080 Tunis, Tunisia

B. Goldschmidt
Département Recherche Appliquée, Groupe - Fromageries Bel, 7 bd de l'industrie, 41100 Vendôme, France

P. Lesieur (✉)
Faculté des Sciences, Université Henri Poincaré, UMR 7565, 54506 Vandœuvre-lès-Nancy Cedex, France
e-mail: pierre.lesieur@uhp-nancy.fr

Introduction

Processed cheese spreads are oil-in-water (O/W) emulsions in a gel state consisting in a proteolipidic network including an aqueous phase which contains salts and dispersing fat droplets. They are sold in most countries whatever the local climate. Thanks to their preparation recipe and process, they are considered to be stable products from a microbiological point of view with a reasonable shelf life. Processed cheese spreads are produced by blending, heating and vigorous stirring of a mixture of shredded natural cheeses of different types and degrees of maturity with chelating (or melting) salts and fat under partial vacuum and constant stirring until a homogeneous mass is obtained [1]. Modern processing technologies may also use various other ingredients to reduce costs, provide flavor or texture, or improve the shelf life. A second type of processed cheese spread is based on a processed cream formula. In this case, the natural cheeses are replaced by a fresh curd mass and cream is added. Melting salts are also added to the blend, but may be different of those used above.

During manufacture of processed cheese spreads, some water is added to produce a smooth and stable emulsion [2]. Water helps in hydrating the proteins and dispersing the components. Water is also required to achieve certain product attributes such as softness in cheese spreads. The amount of water added differs according to whether the product is a full-fat or a low-fat product. Commercial full-fat processed cheese spreads have mass contents of moisture and fat in the 40–60% range and of 16–20% at least, respectively [3–5]. However, commercial low-fat processed cheese spreads (10–24 mass% fat) have been found to contain as much as 73 mass% moisture [6].

Until now, few studies have been carried out on characterization of water properties in this kind of food

structure. Most investigations on exudation or syneresis and methods for measuring water-holding capacity have been carried out on curd [7, 8]. More recently, Marcheseau and Cuq [9] have studied the change in water-holding capacity during processed cheese storage by using ultracentrifugation methods. However, no work has been reported on thermal behaviour of water in processed cheese previously described as a complex system [10].

According to food freezing literature, water may be distinguished into two types with respect to its aptitude to freeze. On one hand, the "free" or "bulk" water, also called "freezable" water, freezes at few degrees below 0 °C, due to a phenomenon of nucleation, but melts either at 0 °C in the absence of soluble substances like salts or below 0 °C in the opposite case. This behaviour is typical of homogeneous hydrated systems, the thermotropic phase transition between ice and liquid aqueous solutions being indeed affected by salts. For instance, 20 mass% NaCl shifts the water solid-to-liquid transition temperature down to −20 °C. In the same way, the transition enthalpy variation is known to be lowered in the presence of soluble solutes, typically from 6 kJ mol^{-1} down to 4 kJ mol^{-1} when the transition temperature drops from 0 °C down to −40 °C [11]. On the other hand, water that remains "unfrozen" at temperatures below the equilibrium bulk freezing temperature, i.e., in the presence of ice, is called "unfreezable" and referred to as "bound" water according to Wolfe et al. [12]. However, this notion of bound water versus that of freezable water must be considered with care as suggested by Van der Sman and Boer [13]. Otherwise, it has been demonstrated that some food materials can undergo a glass transition so that a fraction of bulk water may remain unfrozen since it would evolve towards an amorphous glass state rather than crystallized ice [12, 13]. Because of the frequent concomitance of these different behaviours, the study of water state in processed cheese including quantified identification is complex.

The main goal of the present study was to characterize water state in processed cheese spreads in relation with the microstructure. Few techniques allow both the discrimination and quantification of the different types of water in materials. Among these techniques, Differential Scanning Calorimetry (DSC) can directly measure ice melting/freezing temperatures and enthalpies in foods and other systems [14]. DSC easily provides evaluation of the freezable water amount and that of water molecules which are unable to crystallize due either to specific interaction with the studied matrix or to other processes. Namely, the amount of water that freezes during cooling of a food sample is commonly and easily determined from the melting enthalpy of ice formed under the experimental conditions used [15, 16], especially in the case of inhibited or difficult water crystallization. Here, the aqueous phase of two different cheese matrices obtained by varying composition and manufacturing process was investigated by monitoring the thermal events associated to the freezing of water and melting of ice by DSC. This study was complemented by Environmental Electron Scanning Microscopy (ESEM) observations to visualize the organization as well as the distribution of fat and aqueous phase within the emulsions constituting the processed cheese spreads examined.

Materials and methods

Processed cheese products

Two different processed cheese spreads were provided by the French industrial dairy company Fromageries Bel (Vendôme, France) and selected as representative of two important technologies differing by ingredients and composition of the final product. Cheese A is a processed cheese spread with a 52 mass% of fat on dry matter basis containing the following ingredients: cheese from cows' milk, butter, skim milk, milk proteins and melting salts. Cheese B is a processed cream cheese spread with a 68 mass% of fat on dry matter basis resulting from another mixture of different ingredients (fresh lactic curd, cream, milk proteins and emulsifiers). The determination of pH, dry matter [17], fat content [18], total nitrogen as protein content [19], lactose [20] and ash [21] contents for both cheeses A and B were provided by the supplier from analyses performed in triplicate (see data in Table 1). The samples were stored at 4 °C prior to analyses. All analyses were conducted on products aged between 1 and 2 months.

Table 1 Acidity and Chemical Composition (mass % of total wet matter) of the processed cheese spreads as a result of three independent series of analysis

Cheese	pH	Total moisture	Fat	Protein	Lactose	Ash
A	5.52 ± 0.01	$56.7 \pm 0.1_5$	22.5 ± 0.2	10.5 ± 0.1	6.80 ± 0.07	3.70 ± 0.01
B	5.40 ± 0.01	52.7 ± 0.2	32.2 ± 0.1	9.0 ± 0.1	2.10 ± 0.01	2.70 ± 0.01

DSC measurements

Calorimetric experiments were carried out using a Perkin-Elmer DSC-7 apparatus (St Quentin en Yvelines, France) supported by Pyris Thermal Analyzing Systems ver 352. Dried nitrogen and air were used to purge the thermal analysis system (head and glove box, respectively) during all the experiments.

Lauric acid (99.95% purity, melting temperature, $T_m = 43.7$ °C; $\Delta H_m = 8.53$ kcal mol^{-1}) was used as standard to calibrate the calorimeter for all cooling and heating scans. The samples of both cheeses, in the range of 16.5–21.0 mg, were first hermetically sealed into aluminum pans (50 μL total volume, Perkin Elmer, France). The whole analysis of a sample was carried out using the same sample-holder and monitoring of water evaporation was conducted as previously described [16, 22–24]. The decrease in water content of each sample throughout a series of recordings was obtained thanks to a very small hole (less than 0.2 mm diameter) made in the pan cover after sealing by a special sharp pin prick [24]. Between two sets of recordings and just after the heating scan, the sample pan was kept in dry atmosphere (dried silica gel) at room temperature over night to allow loss of water. The hole in the sample cap was small enough to ensure that water evaporation during the temperature ramp (from −50 to 45 °C) of a calorimetric scan was negligible compared to that applied between two recordings. The samples were precisely weighed between each set of recordings ($\pm 10^{-5}$ g). The slow dehydration process employed warrants homogeneous elimination of water from the samples.

An empty pan was used as a reference and a DSC analysis of empty pans was recorded prior to the sample measurements in the temperature range in which the thermal events of interest are observed. All thermograms were performed at a rate of ±2 °C min^{-1}. Before each recording set, the samples were first cooled from 25 to −50 °C before two successive heating and cooling runs from −50 to 45 °C and from 45 to −50 °C, respectively. The fat matter was in the liquid state at 45 °C and crystallized upon cooling so that the different thermal events corresponding to lipid melting and crystallization were superimposed all along the experiment. The reported data concerning water crystallization correspond to those obtained during the first cooling scan from 25 °C down to −50 °C. The water sample (1 mg of Millipore ultra pure water) was scanned once in the same conditions.

DSC sample analyses were performed in duplicate for both cheeses with excellent repeatability, but only one series of results corresponding to about 16 cycles will be presented here.

The onset temperatures (T_{Onset}) were taken at the intersection of the baseline with the tangent to the left side of the melting peak or to the right side of the freezing one. The specific heats of water melting were obtained by integrating the area under the peaks by using the DSC apparatus software.

Lyophilization

Lyophilization was carried out as a separate experiment on both types of samples prior to microscopy examination with the aim to get freeze dried samples. Large cheese samples (about 20 × 20 × 15 mm) were placed in a freezer at −70 °C for 8 h, and then lyophilized in a freeze dryer under vacuum for 12 h after initial weighing. The level of residual moisture in lyophilized samples was determined by mass differences.

Environmental scanning electron microscopy (ESEM)

Spread cheese samples (5 × 5 × 3 mm) were examined by using an Environmental Scanning Electron Microscope, XL 30 type ESEM–Quanta (Philips/FEI), at beam voltage of 15 kV and reduce pressure of 0.9 mm Hg. The detection system was a Gaseous Secondary Electron Detector (GSED). Both types of samples, wet and lyophilized ones, were mounted onto stubs using a double-sided adhesive tape. Samples were inserted into the microscopy chamber at 4 °C. Only faces of sample not modified by cutting edge were examined. The working distance between the samples and the detector ranged from 8.8 to 11.3 mm. Air pockets, fat droplets and water-rich areas were identified according to the levels of grey (contrast level). Gas or void volumes usually appear as black regions due to the lack of matter. The fat matter areas are seen in more or less dark grey and always lighter than trapped air. The aqueous phase is characterized by significantly higher intensity.

Results

The composition characteristics of the two processed cheeses studied and referred to as cheeses A and B are reported by Table 1. As expected from initial component mixture, the fat content in cheese B was markedly found higher than in cheese A. While the global moisture of cheese B slightly exceeded that of cheese A, protein, lactose and ash levels appeared smaller. The difference in pH value arose from the use of acid curd in cheese B preparation.

Thermotropic behaviour of water as a function of cheese hydration level

Water crystallization and ice melting temperatures as well as corresponding enthalpy variations were determined by

DSC from cheese A and B samples as a function of their progressive dehydration. Each series of recording was conducted on the same sample aliquot placed into a specially perforated capsule, the water content of which varied from its initial value down to lower values until residual water was no more able to crystallize. Water loss (W_L) was controlled by high precision weighing and expressed as mass% of initial sample mass while hydration level was related to the actual sample mass. The DSC profiles were recorded in the total temperature range explored upon heating scans or cooling scans. Whatever hydration levels of the cheese samples, the lipids constituting the fat fraction exhibited crystallization and fusion processes within the 10–35 °C which were found fully superimposed including onset temperatures, shape and surface area of the thermal peaks (data not shown). This implies that thermal events related to water state transitions did not depend on specific lipid–water interactions as previously noticed [25, 26]. In the following, only the temperature interval corresponding to water events was reported. Fat behavior being out of the scoop of this study was recently published separately [27]. Figure 1 shows representative thermograms of cheese A. DSC cooling curves (Fig. 1a) at water losses smaller than 30% by mass (38 mass% residual hydration) exhibit a single narrow and exothermic peak occurring at temperatures significantly below 0 °C. This depicts supercooling behaviour of the aqueous phase similar to that observed for pure water (Fig. 1a, inset). According to such a process, the liquid state is maintained at low temperatures until it abruptly crystallizes due to homogenous crystal nucleation. It can be noticed that lowering the water content of the cheese proportionally decreases the surface area of the DSC signal as well as the crystallization onset temperature which was found always below that of pure water ($T_{Onset} = -17.2$ °C). At hydration levels lower than 38%, the crystallization temperature continues to be shifted down with decreasing hydration while peak broadening is observed. At remaining 24.4% hydration and below, any exothermic event was no more detected indicating that water was not able to freeze upon the thermal treatment imposed.

Heating curves (Fig. 1b) are characterized by a single asymmetrical endothermic event which systematically occurs over a range of subzero temperatures even for $W_L = 1.0\%$ ($T_{Onset} = -5.8$ °C). The peak widths are larger than that for pure water (Fig. 1b, inset) and temperatures characterizing the onset of the melting transition are clearly below 0 °C. Moreover, both the T_{Onset} values and surface area of the endotherms are progressively decreasing with decreasing water content. At the lowest residual water level analyzed, a very weak endothermic signal was noticed (Fig. 1b) at T_{Onset} of −26 °C, whereas no crystallization was recorded upon cooling. This suggests the existence of a crystallization process too slow to be observed at a cooling rate of −2 °C min^{-1} but fast enough to allow nucleation at −50 °C just before recording heating scan. Furthermore, samples containing lower water amounts showed neither crystallization nor melting processes.

The DSC cooling curves recorded from cheese B appear very comparable to those obtained with cheese A (Fig. 2a), except that no broadening was noticed even at 45.7 mass% of water loss (13.2% of water content). The DSC heating curves are characterized by asymmetrical peaks which are decreased in surface area and shifted down lower temperatures with increasing dehydration (Fig. 2b) as similarly described for cheese A. Below 13.2 mass% water, both water crystallization and ice melting processes were vanished. It can be pointed out that, for a given hydration level, water crystallization and ice melting temperatures in the case of cheese B were found systematically higher than those found in the case of cheese A.

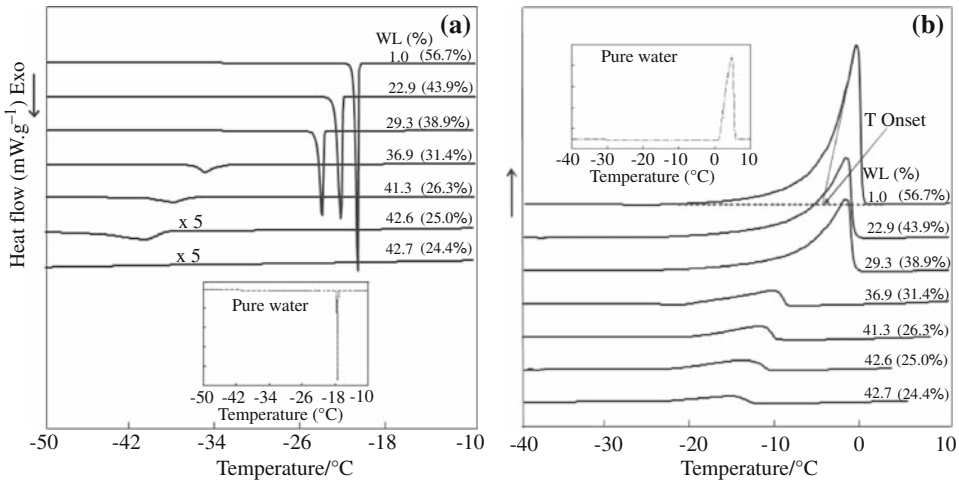

Fig. 1 DSC curves recorded during cooling (**a**) and subsequent heating (**b**) of cheese A at 2 °C min^{-1} as a function of water loss (W_L) expressed in % of the total sample mass. Numbers in parentheses are hydration levels of the samples (% by total sample actual mass). *Insets*: DSC curves of pure water freezing (*a*) and pure ice melting (*b*). Onset temperature T_{Onset} of ice melting were determined as indicated in (b)

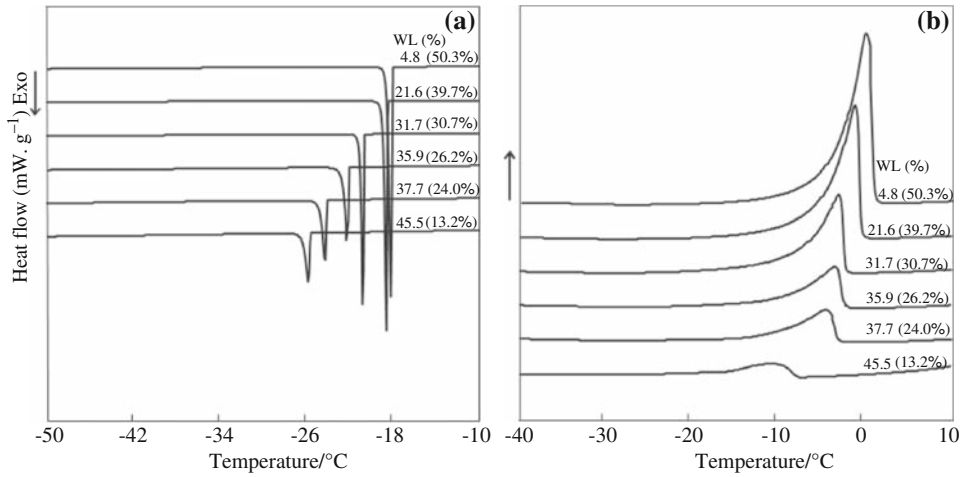

Fig. 2 DSC curves recorded during cooling (**a**) and subsequent heating (**b**) of cheese B at 2 °C min^{-1} as a function of water loss (W_L) expressed in % of the total sample mass. Numbers in parentheses are hydration levels of the samples (% by total sample actual mass)

Figure 3 gathers the evolution of the experimental crystallization and melting temperatures determined for both cheeses as a function of residual water level. It is worth noting that ice formation takes place at temperatures significantly below the melting ones, confirming the supercooling behaviour of water. The temperatures characterizing the solid-to-liquid state transition of water gradually decrease with decreasing hydration level in a close manner for both series of cheese samples. More precisely, looking for instance at the melting temperatures, these are first very slightly decreased with decreasing water content down to 40 and 30 mass% for cheese A and B, respectively. Beyond, successive dehydration steps lead to increasingly significant lowering of the onset temperature.

The variation of the specific heat (ΔH in J g^{-1}) associated with the transition of ice to liquid aqueous solution and measured upon ice melting was plotted in Fig. 4 as a function of the water mass remaining in the samples. As a whole, ΔH values found for water in cheeses are significantly lower than the enthalpy variation of 334.5 J g^{-1} for pure water melting in similar DSC recording conditions. At a given water amount, the value measured for cheese A was systematically below that found for cheese B. For both cheeses and by decreasing hydration, the specific heat is first slightly before abruptly decreasing, thus depicting a change in water ability to freeze. Both parts of the ΔH versus water curves can be rationally assimilated to straight lines. The intercept of these lines gives an estimate of the sample hydration threshold that delimits the two water behaviors and found around 40 or 37 mass% of initial water (32 or 28% mass of total sample) for cheese A or B. In principle and as already experimented [24], the extrapolation to zero ordinate should give the amount of water which is unable to freeze. Indeed, zero ΔH value indicates that no more water could crystallize in the samples during cooling so that no melting event could be observed. By fitting the experimental points by an empiric polynomial law and determining the intercept at zero ordinate, estimates of the critical water contents were found nearly at 19 and 15% by mass of the initial water constituting cheeses A and B, respectively. The impediment to crystallization may be due to interactions with the hydrophilic components of the cheeses, i.e., lactose, proteins and mineral salts (ashes) the proportions of which are given in Table 1. Calculations indeed lead to global hydrophilic substances amount of 4.3 mg in cheese A against only 2.0 mg for cheese B, in agreement with the greater proportion of water that can not freeze in cheese A.

Cheese microstructure characterization

Environmental scanning electron microscopy micrographs of cheeses A and B in their initial hydration state are shown in Fig. 5. Fat droplets (FD) are mainly seen as individual

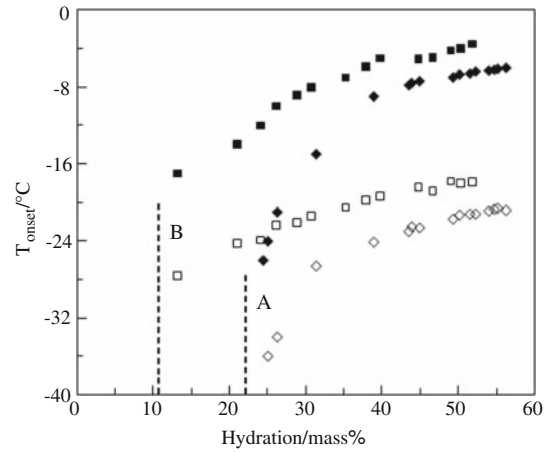

Fig. 3 Plots of onset freezing (*open symbols*) and onset melting (*filled symbols*) temperatures (T_{Onset}; ±0.8 °C precision) characteristic of water contained in cheese A (*diamond symbols*) and cheese B (*square symbols*) versus water fraction expressed as mass% of total sample. *Vertical lines* indicate the hydration levels from which DSC signal was no more detected

spheroids appearing as dark grey spots of variable size. More precisely, in cheese A, the fat droplets typically do not exceed 1 µm in mean diameter (Fig. 5a) while in cheese B, they present a larger size distribution and tend to form clusters (AFD, Fig. 5b, c) which can fuse into non-globular fat domains (NGF) also called "free" fat domains (Fig. 5c). These last are no more protected by the milk original fat globule membrane and correspond to the ultimate step of emulsion destabilization [28].

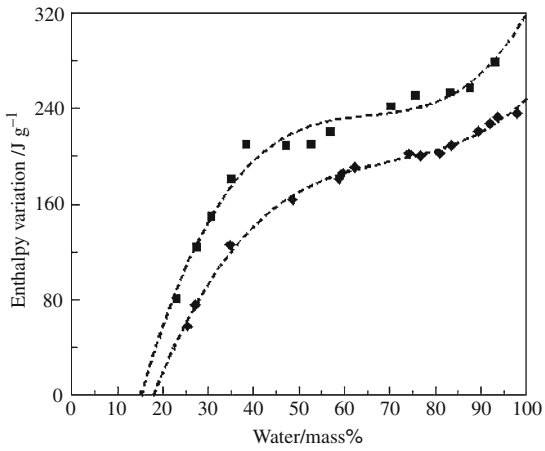

Fig. 4 Enthalpy variation (ΔH in Joules per gram of water, ±8 to ±13 J g^{-1} precision) measured upon ice melting as a function of water expressed as the percentage of initial water mass for cheese A (*diamond symbols*) and B (*square symbols*). *Dashed curves* correspond to the best polynomial fitting of the experimental points ($R = 0.99$)

According to these observations, cheese A shows a degree of fat emulsification higher than that of cheese B. For both matrices, the fat droplets are dispersed and entrapped in a protein network revealed as a light grey background surrounding the fat globules and mainly composed of caseins [29]. The proteins are found close or within the aqueous phase domain that also contains water-soluble salts and lactose (Table 1) and do not totally seem to be uniformly distributed but partly aggregated at a micrometer scale as depicted by the presence of dark small grains beside areas almost white (Fig. 5a, b). The water-rich fraction then appears unlike a homogenous aqueous phase. Moreover, the very light domains can be attributed to water-rich areas which then are clearly localized as larger surface domains in cheese B than seen in cheese A.

Micrographs shown in Fig. 6 exemplify the microstructure of cheeses A and B after freeze-drying and then containing residual water contents of 7.1 and 3.5% by mass, respectively. It is worth noting that this dehydration procedure avoided sample heating. According to DSC analysis performed on both lyophilized samples (data not shown), no water crystallization and subsequent fusion could be detected upon repeated cooling and heating scans in the −50 to 40 °C range. For both samples, dehydration leads to the formation of cracks similar in shape but larger in the case of cheese B (Fig. 6a, c), with lengths not exceeding a 100 µm for cheese A and reaching several hundreds of micrometers for cheese B. The structures of the cheese matrices seen at higher magnification (Fig. 6b, d) closely resemble those characterizing the hydrated samples

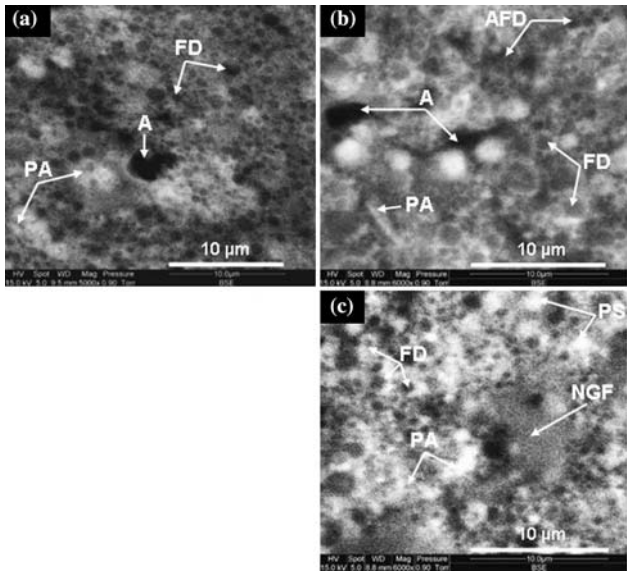

Fig. 5 Scanning electron micrographs of cheeses A (**a**) and B (**b**, **c**). *FD* fat droplets, *A* air pockets, *PA* protein aggregates, *AFD* aggregated fat droplets, *NGF* non globular fat. **b** and **c** micrographs visualize different zones of the same sample

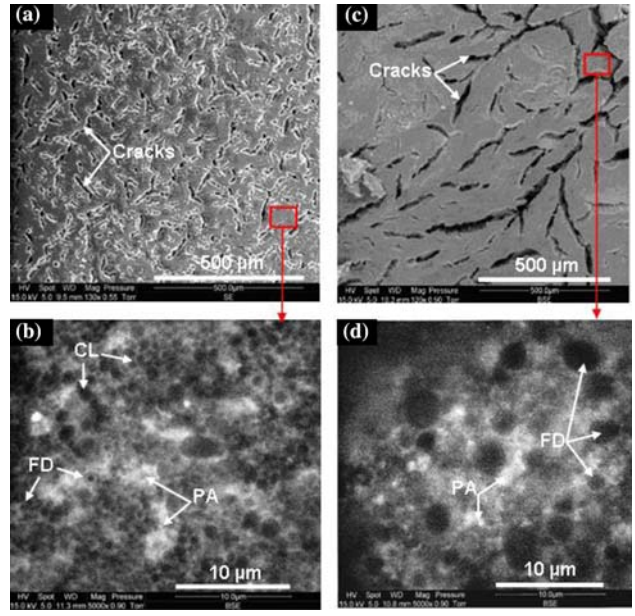

Fig. 6 Scanning electron micrographs of cheeses A (**a**, **b**) and B (**c**, **d**). *FD* fat droplets, *PA* protein aggregates, *CL* clusters of aggregated fat globule. Water contents are 7.1 mass% (**a**, **b**) and 3.5 mass% (**c**, **d**)

(Fig. 5a, b) except that the surface density of the fat droplets tends to increase in both cheeses and more fat coalescence is observed in cheese B. In summary, before dehydration, fat globules have a smaller size in cheese A while after dehydration they appear more coalesced in cheese B.

Discussion

According to above-described chemical analysis and microscopy results, the two processed cheese spreads here studied present a commonly observed matter organization consisting in emulsion fat droplets distributed within an aqueous phase including proteins, lactose and mineral salts. Precise characterization of the aqueous compartment can be achieved through the continuous exploration of water thermal behaviour as a function of controlled cheese dehydration. This has been indeed successfully demonstrated for the study of surfactant-water or polymer-water systems [23, 24].

From the structural point of view, ESEM investigation reveals significant differences between cheeses A and B. Both of them show fat droplets embedded in a hydrated matrix rich in proteins. On the basis of previous reports [4, 29, 30], proteins in milk are principally caseins which localize at the fat/water interface or form individual micelles, and serum proteins which are water-soluble and then mixed with lactose and salts. The fat droplets are surrounded by protein shells directly in contact with the bulk aqueous solution. From images of native samples seen in Fig. 5, cheese A presents particles with smaller sizes and lower polydispersity than those observed for cheese B. It can be reasonably predicted that the network of the water molecules extends into micro-domains with volumes of local dimensions lower in cheese A than in cheese B. Moreover, the latter is partially composed of non-dispersed fat then with the risk of water demixing. Upon gentle freeze-drying that preserves the overall fat organization, Fig. 6 clearly indicates that water loss induces tighter packing of the fat droplets without drastically changing their number and size. As a consequence, cheese dehydration should essentially act on the extent of the aqueous spaces and therefore on the local concentration not only of proteins but also of lactose and mineral salts. In this way, smaller and rather calibrated droplets like those of cheese A should delimit numerous small pockets of aqueous phase which could be separated from each other by eliminating water. In the case of cheese B, the presence of larger globules should lead to wider aqueous areas and may shift the occurrence of restricted domain formation. When cooling, ice crystal growth from a seed can drive larger amounts of surrounding water in cheese B than in cheese A, in good agreement with the distribution of the cracks visualized by ESEM after ice sublimation process. Indeed, these cracks are provoked by sample lyophilization and cannot only coincide with ice localization.

The DSC results provide further information on the aqueous phase. In the operating conditions used, pure water underwent a typical supercooling process. Ice crystallization was indeed observed at −18 °C, i.e., well below the standard temperature of 0 °C, and characterized by the vertical right side and narrowness of the thermal peak. As expected, the melting of the ice crystals in equilibrium with pure liquid water was observed at 0 °C [11]. Both cheeses similarly showed supercooling phenomenon and ice crystallization was shifted at subzero temperatures which were all the lower as the water content is decreased and far below the crystallization temperature observed for pure water. The downshift of ice freezing temperature compared to ice melting one is also an evidence of supercooling. On one hand, this behaviour suggests that within the cheeses, ice forms according to a mechanism of homogenous nucleation, a seed crystal being required to allow the crystal structure to develop in the whole aqueous compartment. On the other hand, the fact that the depressions of the freezing point as well as that of the melting point depend on the hydration level or, more precisely, on the solute concentration, refers to colligative properties of water. This is a direct consequence of the Raoult law which predicts that the addition of a liquid-soluble but solid-insoluble solute to water only lowers the chemical potential of the solvent in the liquid solution. Thus, the temperature of the solid to liquid solution transition is decreased. Consequently, the melting point of the solid in the presence of liquid supplemented by a solute is less than that of the pure compound. Moreover, at-equilibrium freezing point depression is proportional to the solute concentration, at low ones at least. The cheeses here studied contain proteins, lactose and salts which can be, at least partly, dissolved in water so that on cooling the constitutive aqueous solutions do not freeze at 0 °C but at lower temperatures which fit the melting point line referred to as *liquidus* line in the solute-water phase diagram. Ice formation consumes pure water and results in a more concentrated solution that will freeze at an even lower temperature. In the absence of supercooling, melting and freezing pathways are undistinguishable and crystallization should appear as a non-isothermal transition until complete solidification of water. This generally takes place through a eutectic reaction at a very low temperature. The shape of the temperature variation seen in Fig. 3 strongly suggest the existence of such an eutectic behaviour which should occur below −50 °C in agreement with the state diagram of water milk previously established [31]. As both cheeses exhibit supercooling, DSC cooling recordings under-estimate the effective transition temperature and yield exothermic

events out of equilibrium. The crystallization exotherms remain narrow as if isothermal transitions were present although this is due to the sudden transformation of the metastable liquid into ice. Only the heating pathway, which is not affected by any nucleation process, must be considered to closely describe the state diagram of the aqueous fraction of the cheeses. This last clearly shows expected non-isothermal melting since the peak width significantly exceeds that observed for pure water. In this respect, both cheeses behave similarly and present eutectic-like behaviour, the limit of the *liquidus* line at low water content being symbolized by the vertical dashed lines in Fig. 3. The shift between the two cheese samples can be first explained by the different amount of hydrophilic substances they contain which is almost twice higher for cheese A (Table 1). The influence of the proportions of the hydrophilic substances, namely the lactose proportion, and possibly of the nature of the constitutive proteins and/or mineral salts cannot be either excluded.

By reconsidering more carefully the shape of the exothermic peaks characteristic of ice formation, those at low water contents deserve attention. They indeed reveal a discrepancy between cheeses A and B. As exemplified by Fig. 7, cheese A shows progressive water freezing along a rather wide temperature range as if crystals would not cooperatively grow from initial nuclei what is exactly the case for cheese B. By taking into account that water in both cheeses undergo supercooling and in agreement with ESEM analysis, a reasonable explanation could be that the decrease in the distance between fat droplets upon water elimination creates, in cheese A, aqueous zones of likely variable concentrations and/or compositions which do not communicate anymore and then behave independently. Each small domain then would freeze from its own supercooled state at a temperature different from the other ones, however, close enough to be not discriminated by the DSC apparatus.

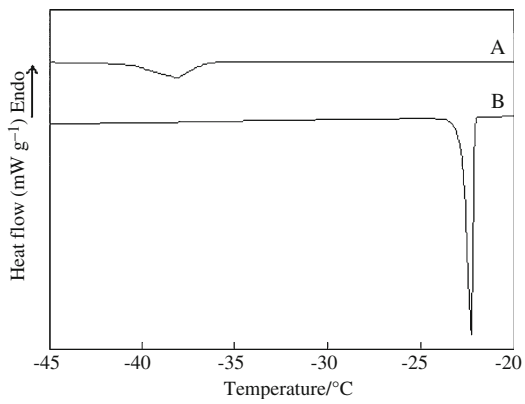

Fig. 7 DSC curves recorded at 2 °C min^{-1} during cooling of cheeses *A* and *B* containing 26.3 and 26.2% water by mass of total sample, respectively

Moreover, water crystallization in cheese A is systematically delayed compared to cheese B. This may be again related to the existence of the more reduced water spaces within the matrix of cheese A, in agreement with previous observations concerning water-in-oil emulsions, for which the smaller the size of water droplets and the higher their salt concentration, the lower the freezing temperature [29, 32]. Another superimposed phenomenon may be the reduction of ice crystal growth in cheese A, due to very small volumes of liquid water available in the vicinity of the nuclei [33].

The evolution of the specific heat measured during heating DSC scans and associated with ice melting shows two-step behaviour of water in both cheeses depending on the hydration level. The overall ΔH value per gram of water remains lower than 240 or 290 J g^{-1} for cheese A or B, respectively. These values are plainly below the enthalpy variation of ice melting for pure water. It is worth noting that melting heat of 334 J g^{-1} corresponds to the ice-to-liquid water transition occurring at 0 °C so that it could be expected lower at temperatures significantly colder due to differences in the heat capacities of ice (close to 2 J g^{-1} K^{-1}) and liquid water (close to 4 J g^{-1} K^{-1}) versus temperature. Another factor is the presence of the water-soluble compounds lactose, proteins and mineral salts. Indeed, upon heating, the energy exchange by water in the cheeses is the sum of two contributions: the energy required by the ice-to-liquid transition and the energy corresponding to the solubilisation of the hydrophilic substances into the liquid water. Ice melting is an endothermic event (positive enthalpy variation) and in the hypothesis of pure ice crystallization, it should be equal to that of pure water (334 J g^{-1}) and the related heat exchange directly proportional to the water mass. Solute solubilisation is spontaneous and probably contributes to lower overall enthalpy variation for both cheeses. Presently, cheese A which contains more soluble species exhibits lower enthalpy changes. This is in favour of an effect associated to the solubilisation of lactose, proteins and salts. Solute solubilization corresponds to negative free energy variation. However, depending on the nature of the solutes, the event is either exothermic (negative enthalpy variation) or endothermic (positive enthalpy variation). In the latter case the enthalpy variation is compensated by entropy variation. Whatever the solubilisation behaviour, the exchanged heat is proportional to the solute concentration and then varies with the water content. The fact that the specific melting heat was found below that of pure water and progressively decreased with decreasing water mass suggests that solute solubilisation may be exothermic rather than endothermic. An alternative explanation may be partial water freezing upon sample cooling so that the recovered melting enthalpy variation

reduced to the total water mass may be found systematically lower than that expected if all the water would have crystallized.

At high dehydration, below around 30 mass% total sample (from around 5 mg and 3 mg water in cheese A and B, respectively), the significant decrease in enthalpy variation measured during cheese heating process confirms that part of the constitutive water molecules did not crystallize upon the preceding cooling down to −50 °C. The critical water contents deduced from extrapolation to zero enthalpy (Fig. 4), reduced to the hydrophilic components of cheeses, amount to very close mass fractions of either 34% (cheese A) or 36% (cheese B), i.e., a quite similar solute mass fraction of 65%. Logically this composition can be assimilated to that of the expected eutectic-like mixture corresponding to the coexistence between liquid aqueous solution, ice and a glassy solid state as supported by previous works [12, 31]. While ice is, theoretically and at equilibrium, constituted by pure water, the glass state is issued from a viscous aqueous liquid composed of water and hydrophilic species. Upon dehydration strong solute–water interactions develop to the detriment of water–water interactions and hinder water crystallization. Another possible reason is the increase in viscosity catalyzed by dehydration and cooling which impedes the diffusion and gathering of the water molecules required for the freezing process. It should be pointed out that in the present study, no glass transition could be recorded during either cooling or heating DSC measurements. This may be explained first by a very low temperature of such a glass transition that have been already found either at −80 °C in cheese curds [34] or in the −64 to −69 °C range for fresh cheeses [35]. Then the glassy solid formation in cheeses A or B would not occur at −50 °C. The fact would be that the water molecules "bounded" to the hydrophilic substances would remain in a liquid-like state unable to freeze. The second explanation may be related to the low glass-to-liquid relaxation enthalpy [34] that would be not measurable by the DSC apparatus we used. From a practical point of view, these results as a whole show that the moisture in both cheeses splits into two water states: free water molecules which act as a solvent of part of the hydrophilic solutes (proteins, lactose and mineral salts) and hydration water which tightly interacts with the hydrophilic solutes to form hydrate-like structures. At high hydrations, free water freezes at relatively moderate temperatures then at moderate viscosities and ice formation, which is energetically favorable, manages to draw the hydration water so that most or all water crystallizes. At low content, water becomes more confined and the viscosity increases so that free water molecules hardly diffuse. Freezing is delayed and the hydration water is retained in the vicinity of its neighboring molecules and cannot organize to produce ice. This confinement effect is especially ascertained for cheese A. Moreover, ESEM experiments performed after sample heating for different periods of time (data not shown) showed that while cheese B underwent partial coalescence of the fat droplets, cheese A was not significantly modified. Trend of cheese B to demixing, at the opposite of cheese A that conserves its microstructure, strengthens thermal behavior interpretation in terms of fragmentation of the aqueous phase and network tortuosity.

Conclusions

Very little information about water behavior in processed cheese spreads had been previously reported likely due to the complexity of their composition and structural organization. This study is a first attempt to characterize the moisten fraction of these food materials by combining ESEM and DSC. Despite rather middle resolution, ESEM technique revealed convenient to describe the microstructure of cheese matrices in their native hydration state. The images clearly reported a dispersion of fat globules distributed within an aqueous network composed of partially crystallized proteins. DSC analysis on samples submitted to gentle and progressive dehydration was particularly informative. It highlighted that the moisten continuum corresponds to an aqueous solution of the cheeses hydrophilic components, i.e., lactose, salts and proteins, a part of the water molecules being unable to freeze even at −50 °C. The thermal behavior of water was sensitive to the connectivity of the aqueous network and permits to distinguish cheese emulsions differing by the size distribution of the fat globules. As indeed confirmed by direct ESEM visualization, the more significant the delay of water freezing and the less cooperative the nucleation-growth process of ice crystals, the smaller the fat droplets and the more developed the array of water channels apt to form isolated micro-domains. At this stage of interpretation, it would be interesting to complete the structural approach by NMR analyses very recently reviewed as a powerful tool to deepen food microstructure [36]. This will be the subject of a further work. DSC coupled to controlled dehydration thus provides an interesting and simply implementable method to identify the micro-organization of processed cheese spread, mainly implicated in the textural properties of these products.

Acknowledgements We gratefully acknowledge Mr. Abdessalem Harrabi and Ms. Fatma Masmoudi for assistance in the use of ESEM technique (service commun d'analyses de l'INRST, Borj Cedria, Tunisia).

References

1. Paquet D. Processed cheeses: physico-chemical aspects. In: Lorient D, Colas B, Le Mestre M, editors. Functional properties of food macromolecules. Les cahiers de l'ENSBANA. Paris: Technique & Documentation Lavoisier; 1988. p. 227–41.
2. Berger W, Klostermeyer H, Merkenich K, Uhlmann G. Processed cheese manufacture. Ladenburg: BK Ladenburg GmbH; 1993.
3. Chang PK. Process cheese containing a modified whey solids. US Patent 4166142 1979.
4. Caric M, Kalab M. Processed cheese products. In: Fox PF, editor. Cheese: chemistry, physics and microbiology, vol. 2. London: Chapman & Hall; 1993. p. 467–505.
5. Hockenberry TM, Evanston AJM (1994) Method for continuous manufacture of process cheese-type products, US Patent 5350595.
6. Lee SK, Klostermeyer H. The effect of pH on the rheological properties of reduced-fat model processed cheese spreads. LWT-Food Sci Technol. 2001;34:288–92.
7. Marshall RJ. An improved method for measurement of the syneresis of curd formed by rennet action on milk. J Dairy Res. 1982; 49:329–36.
8. Kocher PN, Foegeding EA. Microcentrifuge-based method for measuring water-holding of protein gels. J Food Sci. 1993;58: 1040–6.
9. Marchesseau S, Cuq JL. Water-holding capacity and characterization of protein interactions in processed cheese. J Dairy Res. 1995;62:479–89.
10. Meyer A. Processed cheese manufacture. London: Food Trade Press; 1973.
11. Franks F. The properties of aqueous solutions at subzero temperatures. In Franks F editor. Water, a comprehensive treatise. New York: Plenum Press; 1982. p. 215–338.
12. Wolfe J, Bryant G, Koster KL. What is 'unfreezable water', how unfreezable is it, and how much is there? CryoLetters. 2002; 23:157–66.
13. Van der Sman RGM, Boer E. Predicting the initial freezing point and water activity of meat products from composition data. J Food Eng. 2005;66:469–75.
14. Farkas J, Mohacsi-Farkas C. Application of differential scanning calorimetry in food research and food quality assurance. J Therm Anal Calorim. 1996;47:1787–803.
15. Pouchly J, Biros J, Benes S. Heat capacities of water swollen hydrophilic polymers above and below 0 °C. Makromolekulare Chemie. 1979;180:745–60.
16. Ollivon M. Calorimetric and thermodielectrical measurements of water interactions with some food materials. In: Levine H, Slade L, editors. Water relationships in foods. Advances in the 1980s and trends for the 1990s. New York & London: Plenum Press; 1991. p. 175–89.
17. ISO 5534. Fromages et fromages fondus—Détermination de la teneur totale en matière sèche (Méthode de référence), International Organization of Standardization; 2004.
18. ISO 3433. Fromages—Détermination de la teneur en matière grasse—Méthode acido-butyrométrique, International Organization of Standardization; 2002.
19. IDF-FIL 20-1. Lait. Détermination de la teneur en azote. Partie 1: Méthode Kjeldahl, International Dairy Federation; 2001.
20. ISO 22662. Lait et produits laitiers Détermination de la teneur en lactose par chromatographie liquide haute performance. Méthode de reference, International Organization of Standardization; 2007.
21. NF V04-208. Lait- Détermination des cendres. Méthode de référence. French Association of Normalization; 1989.
22. Seras M, Courtois B, Quinquenet S, Ollivon M. Measurement of the complex permittivity of dielectrics during microwave heating: study of flours and starches. In: Jowitt R, Escher F, Kent M, McKenna B, Roques M, editors. Physical properties of foods-2, New York & London; 1987. p. 217–23.
23. Kekicheff P, Grabielle-Madelmont C, Ollivon M. Phase diagram of sodium dodecyl sulfate-water system: 1. A calorimetric study. J Colloid Interface Sci. 1989;131:112–32.
24. Cansell F, Grabielle-Madelmont C, Ollivon M. Characterization of the aqueous phase and the water-polymer interface in latex suspensions by differential scanning calorimetry. J Colloid Interface Sci. 1991;144:1–17.
25. Bazmi A, Relikn P. Thermal transitions and fat droplet stability in ice-cream mixmodel systems: effect of milk fat fractions. J Therm Anal Calorim. 2006;84:99–104.
26. Thanasukarn P, Pongsawatmanit R, McLement D. Impact of fat and water crystallization on the stability of hydrogenated palm oil-in-water emulsions stabilized by whey protein isolate. J Colloids Surf A. 2009;246:49–59.
27. Gliguem H, Ghorbel D, Lopez C, Michon C, Ollivon M, Lesieur P. Crystallization and polymorphism of triacylglycerols contribute to the rheological properties of processed cheese. J Agr Food Chem. 2009;18:3195–203.
28. Lopez C. Focus on the supramolecular structure of milk fat in dairy products. Reprod Nutr Dev. 2005;45:497–511.
29. Fox PF, Guinee TP, Cogan TM, McSweeney PH. Fundamentals of cheese science. Gaithersburg, Maryland: ASPEN Publishers; 2000.
30. Marchesseau S, Gastaldi E, Lagaude A, Cuq JL. Influence of pH on protein interactions and microstructure of process cheese. J Dairy Sci. 1997;80:1483–9.
31. Vuataz G. The phase diagram of milk: a new tool for optimising the drying process. Lait. 2002;82:485–500.
32. Clausse D, Gomez F, Pezron I, Komunjer L, Dalmazzone C. Morphology characterization of emulsions by differential scanning calorimetry. Adv Colloid Interface Sci. 2005;117:59–74.
33. Aguerd M, Babin L, Clausse D. Contribution à l'étude de la nucléation spontanée et induite des phases aqueuses dispersées. J Rech Atmos. 1984;18:131–4.
34. Béal C, Fonseca F, Thomas A, Marin M. Caractérisation et lyophilisation de matrices fromagères. Sci Alim. 2006;26:89–102.
35. Andersen AB, Hansen E, Jorgensen U, Skibsted LH. Glass transition in frozen fresh cheese. Milchwissenschaft-Milk Sci Int. 2001;56:441–3.
36. Mariette F. Investigations of food colloids by NMR and MRI. Curr Opin Coll Int Sci. 2009;14:203–11.